Physica B 404 (2009) 1840–1846

Contents lists available at ScienceDirect

Physica B

journal homepage: www.elsevier.com/locate/physb

Layered growth model and epitaxial growth structures for SiCAlN alloys

Zhaoqing Liu [a], Jun Ni [a,*], Xiaoao Su [b], Zhenhong Dai [b]

[a] Department of Physics and Key Laboratory of Atomic and Molecular Nanoscience (Ministry of Education), Tsinghua University, Beijing 100084, PR China
[b] Department of Physics, Yantai University, Yantai 264005, PR China

ARTICLE INFO

Article history:
Received 15 May 2008
Accepted 2 March 2009

PACS:
81.10.Aj
61.50.Ah
74.70.Dd
71.20.Nr

Keywords:
Layered growth
Epitaxial growth
Phase diagram
SiCAlN alloys
Polytype
First-principle calculation

ABSTRACT

Epitaxial growth structures for $(SiC)_{1-x}(AlN)_x$ alloys are studied using a layered growth model. First-principle calculations are used to determine the parameters in the layered growth model. The phase diagrams of epitaxial growth are given. There is a rich variety of the new metastable polytype structures at $x=\frac{1}{6},\frac{1}{5},\frac{1}{4},\frac{1}{3}$, and $\frac{1}{2}$ in the layered growth phase diagrams. We have also calculated the electronic properties of the short periodical SiCAlN alloys predicted by our layered growth model. The results show that various ordered structures of $(SiC)_{1-x}(AlN)_x$ alloys with the band gaps over a wide range are possible to be synthesized by epitaxial growth.

1. Introduction

(SiC)–(III-N) alloys, as wide-band-gap semiconductors, are promising materials for microelectronic and optoelectronic applications. Among these alloys, SiCAlN alloys have been extensively studied because they have the full miscibility at temperatures above 1700 °C and the band gaps over a wide range with the change of the composition [1].

In recent years, there are many experiments to fabricate SiCAlN alloys. Early attempts of fabricating ceramic alloys in SiC–AlN system use hot-pressing of powders at very high temperature in the range of 1700−2100 °C generally [2,3]. Later $(SiC)_{1-x}(AlN)_x$ solid-solution films are grown by plasma-assisted gas source molecular beam epitaxy (MBE) [4–6] and metal organic chemical vapour deposition (CVD) [7,8] between 1000 and 1300 °C. Lately the growth of single-phase SiCAlN epitaxial films is accomplished by MBE at substrate temperature of 500−750 °C [9–13]. The periodic SiC/AlN multilayered structure has been grown by low pressure CVD [14].

Previous calculations on SiCAlN alloys are mostly performed using $(SiC)_{1-x}(AlN)_x$ solid-solution models with the crystal structure of hexagonal wurtzite [11–13] or zinc-blende [15]. Recently, the ordered wurtzite structural model for $(SiC)_{1-x}(AlN)_x$ ($x=0.00$, 0.25, 0.50, 0.75, and 1.00) has been used to study their electronic structures by Tang et al. [16]. The properties of SiCAlN structures composed of SiC and AlN polytypes have been investigated by first-principle calculations [17]. Their electronic properties vary from wide-band-gap semiconducting to metallic.

However, there are seldom theoretical works to simulate the growth of SiCAlN alloys. The possible epitaxial structures of SiCAlN are still remaining unknown. Modelling of epitaxial structures would be helpful for the experimental synthesis. In this paper, we have predicted the epitaxial growth structures of SiCAlN alloys by an layered growth model. We have also obtained the phase diagrams of epitaxial growth, which show that 3C–SiC, 4H–SiC, $(SiC)_{5/6}(AlN)_{1/6}$, $(SiC)_{3/4}(AlN)_{1/4}$, $(SiC)_{2/3}(AlN)_{1/3}$, $(SiC)_{1/2}(AlN)_{1/2}$, and 2H–AlN are likely to be formed during epitaxial growth.

The paper is organized as follows. Section 2 describes the methods. In Section 3 we first show the layered growth phase diagrams and the corresponding phase structures, and then the electronic properties of the short periodical SiCAlN alloys predicted by our layered growth model. The conclusions of this work are presented in Section 4.

2. Methods

SiC and AlN both exhibit polytypism. Among more than 200 different polytypes of SiC [18], the most common ones are 3C–SiC

* Corresponding author. Tel.: +8610 62772781; fax: +8610 62781604.
E-mail address: junni@mail.tsinghua.edu.cn (J. Ni).

0921-4526/$ - see front matter © 2009 Elsevier B.V. All rights reserved.
doi:10.1016/j.physb.2009.03.001

(zinc-blende), 2H–SiC (wurtzite), 4H–SiC, 6H–SiC, and 15R–SiC. The band gap of SiC ranges from 2.403 eV for 3C–SiC to 3.33 eV for 2H–SiC [19,20]. AlN usually has hexagonal wurtzite structure, but it has also been reported to be stabilized in the zinc-blende structure [21,22]. 4H–AlN and 6H–AlN polytypes have been grown by MBE [23–26].

All the SiC (or AlN) polytypes could be considered as different arrangements of hexagonal or cubic Si–C (or Al–N) bilayers by stacking along the hexagonal [0 0 0 1] or equivalent cubic [1 1 1] direction geometrically. 2H–SiC (or AlN) is the pure hexagonal stacking of Si–C (or Al–N) bilayers in the [0 0 0 1] direction and 3C–SiC (or AlN) is the pure cubic stacking of Si–C (or Al–N) bilayers in the [1 1 1] direction. The other polytypes such as *n*H–SiC (or AlN) or *n*R–SiC (or AlN) in the Ramsdell notation [27] can be considered as combinations of the two stacking sequences of the *n*Si–C (or Al–N) bilayers in the primitive cell. In the Hägg notation [28], each bilayer that can be stacked in two possible orientations on the underlayer is labelled with the symbol $s_i = \pm 1$. With this notation, the polytypes 3C, 2H, 4H, and 6H can be represented as a repetition of $++-$, $+-$, $++--$, and $++-+--$ unit cells, respectively. In the Zhdanov notation [29], the consecutive $+$ and $-$ signs are summed up and the resulted numbers are used to denote the structures. With this notation, these four polytypes are denoted by symbols $\langle\infty\rangle$, $\langle 11\rangle$, $\langle 22\rangle$, and $\langle 33\rangle$, respectively.

Suggested by the experimental findings [11–13] and our first-principle calculations, the SiCAlN alloy structures in this study have the altering layers with the preferred interface bonding configurations of Si–N and Al–C. One SiC polytype and one AlN polytype stack alternately in each structure along the hexagonal [0 0 0 1] or equivalent cubic [1 1 1] direction. We notate these structures with *n*H(C)*m*H(C) ($n = 2, 3, 4, 6$, and $m = 2, 3, 4, 6$) in which the first Ramsdell symbol denotes the SiC constituent and the second Ramsdell symbol denotes the AlN constituent, for example, 2H2H, 3C2H, 2H3C, and 4H2H denote 2H–SiC/2H–AlN, 3C–SiC/2H–AlN, 2H–SiC/3C–AlN, and 4H–SiC/2H–AlN, respectively. In Fig. 1, we show the atomic configurations in the hexagonal $(1\,1\,\bar{2}\,0)$ plane of some SiCAlN structures. The *n*H(C)*m*H(C) structures can be considered as different arrangements of hexagonal or cubic Si–C and Al–N bilayers by stacking along the hexagonal [0 0 0 1] or the equivalent cubic [1 1 1] direction geometrically. With Hägg notation, the SiCAlN alloys 2H2H, 3C2H, 2H3C, and 4H2H can be represented as a repetition of $+A-A+B-B$, $+A+A+A+B-B$, $+A-A+B+B+B$, and $+A+A-A-A+B-B$ unit cells, respectively, in which the $\pm A$ represent Si–C bilayers and the $\pm B$ represent Al–N bilayers.

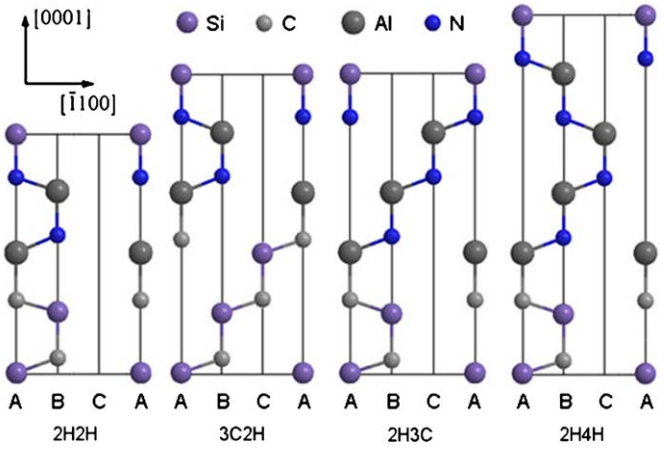

Fig. 1. (Colour online) The atomic configurations in the hexagonal $(1\,1\,\bar{2}\,0)$ plane of some SiCAlN structures.

The one-dimensional stacking sequences of SiC polytypes have been described [30–37] by an axial next-nearest neighbour Ising (ANNNI) model [38–41]. Here we propose a model to represent SiCAlN alloys by extending the ANNNI model. As there are two kinds of bilayers in SiCAlN alloys, we have introduced an lattice gas variable σ_i^α to represent the bilayer species and the chemical potential μ into the ANNNI model. Thus, the Hamiltonian of the SiCAlN system can be represented by

$$H = E_0 - \frac{1}{N}\sum_{\alpha\beta}\sum_i\sum_k J_k^{\alpha\beta}\sigma_i^\alpha s_i \sigma_{i+k}^\beta s_{i+k} + \mu\frac{1}{N}\sum_i(\sigma_i^A - \sigma_i^B), \quad (1)$$

where E_0 is the energy constant, N is the number of the bilayers, and μ is the chemical potential. The label i runs over the bilayers in the unit cell. A "spin" $s_i = \pm 1$ is associated with each bilayer such that the parallel spin represents a locally cubic stacking, and the antiparallel spin represents a locally hexagonal stacking. α (or β) takes values of A and B, which represents Si–C bilayers and Al–N bilayers, respectively. The lattice gas variable σ_i^α represents the ith bilayer species. $\sigma_i^A = 1$ and $\sigma_i^B = 0$ when the ith bilayer is a Si–C bilayer. $\sigma_i^A = 0$ and $\sigma_i^B = 1$ when the ith bilayer is an Al–N bilayer. Thus, each bilayer of SiCAlN alloys is presented with two symbols σ_i^α and s_i. The first symbol represents the bilayer species and the second represents the bilayer stacking orientation. The parameters J_k^{AA} represent the interlayer interactions between two kth nearest neighbouring Si–C bilayers, J_k^{BB} represent the interlayer interactions between two kth nearest neighbouring Al–N bilayers, and J_k^{AB} represent the interlayer interactions between kth nearest neighbouring Si–C and Al–N bilayers. The long-range interactions are small and we restrict the interlayer interactions to the third neighbours ($k \leqslant 3$). Thus the total energies per bilayer of the *n*H(C)*m*H(C) system can be expressed by the interlayer interaction parameters, which are listed in Table 1.

We have performed first-principle calculations using VASP (Vienna ab initio simulation package) [42–45] to obtain the total energies of the *n*H(C)*m*H(C) system which are shown in Table 1. The approach is based on an iterative solution of the Kohn–Sham equations of the Density-Functional-Theory (DFT) in a plane wave basis set with the Vanderbilt ultrasoft pseudopotentials [46]. We use the exchange-correlation functional with the generalized gradient approximation given by Perdew and Wang [47]. We set the plane wave cut-off energy to be 600 eV and the convergence of the force on each atom to be less than 0.01 eV/Å to optimize the lattice constants and the atom coordinates. The mesh of gamma

Table 1
The total energies of the *n*H(C)*m*H(C) system per bilayer represented by the parameters in the layered growth model and calculated by DFT.

SiCAlN	Hamiltonian	E (eV)
2H2H	$E_0 + (J_1^{AA} + J_3^{AA} + J_1^{BB} + J_3^{BB} + 2J_1^{AB} - 4J_2^{AB} + 2J_3^{AB})/4$	−15.06142
2H3C	$E_0 + (J_1^{AA} - 2J_1^{BB} - J_2^{BB} - J_3^{BB} - \mu)/5$	−15.04494
2H4H	$E_0 + (J_1^{AA} - J_1^{BB} + 2J_2^{BB} + 2J_3^{BB} + 2J_1^{AB} - 4J_3^{AB} - 2\mu)/6$	−15.05833
2H6H	$E_0 + (J_1^{AA} - 3J_1^{BB} + 4J_3^{BB} + 2J_1^{AB} - 4\mu)/8$	−15.05707
3C2H	$E_0 - (5J_1^{AA} + 3J_2^{AA} + 3J_3^{AA} - 2J_1^{BB} - J_1^{AB} + J_2^{AB} + J_3^{AB} - 2\mu)/10$	−15.06496
3C3C	$E_0 - (2J_1^{AA} + J_2^{AA} + 2J_1^{BB} + J_2^{BB} + 2J_1^{AB} + 4J_2^{AB} + 6J_3^{AB})/6$	−15.04760
3C4H	$E_0 - (2J_1^{AA} + J_2^{AA} + J_1^{BB} - 2J_2^{BB} - J_3^{BB} + \mu)/7$	−15.05482
3C6H	$E_0 - (2J_1^{AA} + J_2^{AA} + 3J_1^{BB} - 3J_3^{BB} + 3\mu)/9$	−15.05213
4H2H	$E_0 - (J_1^{AA} - 2J_2^{AA} - 2J_3^{AA} - J_1^{BB} - 2J_1^{AB} + 4J_3^{AB} - 2\mu)/6$	−15.07584
4H3C	$E_0 - (J_1^{AA} - 2J_2^{AA} - J_3^{AA} + 2J_1^{BB} + J_2^{BB} - \mu)/7$	−15.05960
4H4H	$E_0 - (J_1^{AA} - 2J_2^{AA} - J_3^{AA} + J_1^{BB} - 2J_2^{BB} - J_3^{BB} - 2J_1^{AB} - 4J_2^{AB} + 2J_3^{AB})/8$	−15.06242
4H6H	$E_0 - (J_1^{AA} - 2J_2^{AA} - J_3^{AA} + 3J_1^{BB} - 3J_3^{BB} - 2J_1^{AB} - 4J_2^{AB} - 2J_3^{AB} + 2\mu)/10$	−15.05738
6H2H	$E_0 - (3J_1^{AA} - 4J_3^{AA} - J_1^{BB} - 2J_1^{AB} - 4\mu)/8$	−15.08814
6H3C	$E_0 - (3J_1^{AA} - 3J_3^{AA} + 2J_1^{BB} + J_2^{BB} - 3\mu)/9$	−15.07233
6H4H	$E_0 - (3J_1^{AA} - 3J_3^{AA} + J_1^{BB} - 2J_2^{BB} - J_3^{BB} - 2J_1^{AB} - 4J_2^{AB} - 2J_3^{AB} - 2\mu)/10$	−15.06985
6H6H	$E_0 - (3J_1^{AA} - 3J_3^{AA} + 3J_1^{BB} - 3J_3^{BB} - 2J_1^{AB} - 4J_2^{AB} - 6J_3^{AB})/12$	−15.06216